

Enhanced quantum communication over Gaussian thermal loss channels using correlated multi-mode thermal states

Kyungjoo Noh^{1,2,*} and Liang Jiang^{1,2}

¹*Departments of Applied Physics and Physics, Yale University, New Haven, Connecticut 06520, USA*

²*Yale Quantum Institute, Yale University, New Haven, Connecticut 06520, USA*

Quantum capacity of a noisy quantum channel characterizes the channel's maximum achievable quantum communication rate (upon optimal quantum error correction or one-way entanglement distillation) and is equal to the regularized coherent information of the channel maximized over all input states. We consider Gaussian thermal loss channels which model loss and gain errors in realistic optical communication channels and microwave cavity modes. The best known lower bound of the quantum capacity of a Gaussian thermal loss channel is the channel's coherent information with respect to a single-mode thermal input state. Here, we provide an improved lower bound of the Gaussian thermal loss channel capacity. Specifically, we introduce a family of correlated multi-mode thermal states which can be efficiently generated by Gaussian Fourier transformation and two-mode squeezing operations. We then show that, in the high loss probability and low input energy regime, such correlated multi-mode thermal states yield larger achievable rates of Gaussian thermal loss channels than the corresponding single-mode thermal state subject to the same average photon number constraint.

Introduction—Quantum error correction or entanglement distillation is essential for reliable transmission of quantum information over a noisy quantum communication channel [1–3]. Quantum capacity of a noisy quantum channel quantifies the maximum amount of quantum information per channel use that can be transmitted faithfully in the limit of infinite channel uses upon an optimal quantum error correction or entanglement distillation scheme [4]. In other words, the quantum capacity of a quantum channel is a fundamental quantity which characterizes the channel's ultimate capability of transmitting quantum information. Thus, evaluation of the quantum capacity of an experimentally relevant quantum channel is of great importance to the quantum information science.

The quantum capacity of a quantum channel can be computed by maximizing regularized coherent information of the channel over all input states [5–7] (see also Ref. [8] for energy-constrained cases). In a special case where a channel is degradable, the maximization of the regularized coherent information can be reduced to the maximization of the one-shot coherent information [9]. Moreover, the one-shot coherent information of a degradable channel is concave in the input states [10] and thus can be efficiently computed by a numerical convex optimization. In another extreme case where a channel is anti-degradable, the channel's quantum capacity equals zero [11].

In general, however, a quantum channel is neither degradable nor anti-degradable. In this generic case, it is essential to maximize the regularized coherent information because coherent information might be strictly superadditive (i.e., the maximum regularized coherent information is strictly larger than the maximum one-shot coherent information) [12–17]. Thus, exact calculation of the quantum capacity of a generic quantum channel is challenging and only lower and upper bounds can be obtained.

Typically, a lower bound of quantum capacity is established by maximizing coherent information over a restricted set of states which are tractable [18], or by designing an explicit quantum error correction scheme and then analyzing its per-

formance [12, 19, 20]. Various methods are available for establishing an upper bound of quantum capacity. Notably, data-processing arguments [21–23] and approximate degradability bounds [21, 24, 25] provided upper bounds of quantum capacities of non-degradable channels which are close to their best known lower bounds.

Gaussian thermal loss channels are particularly important because they model excitation loss and gain errors in realistic optical communication channels and microwave cavity modes. Bosonic pure-loss channels form a subclass of Gaussian loss channels and are either degradable or anti-degradable [11]. Thus, bosonic pure-loss channels are well understood and their quantum capacities are determined analytically [8, 18, 26, 27]. In general, however, a Gaussian thermal loss channel is neither degradable nor anti-degradable [28, 29]. Although there have been several progresses in establishing upper bounds of the quantum capacity of Gaussian thermal loss channels [21–23], its existing lower bound (one-shot coherent information with respect to a thermal input state) [18] has not been improved over the last two decades.

In this letter, we establish an improved lower bound of the Gaussian thermal loss channel capacity than the existing bound. In particular, we construct a family of correlated multi-mode thermal states which can be prepared efficiently by Gaussian Fourier transformation and two-mode squeezing operations. Then, we show that, in the high loss probability and low input energy regime, these correlated thermal states yield larger coherent information (per channel use) of Gaussian thermal loss channels than the corresponding single-mode thermal state.

Gaussian states and thermal loss channels— Consider N bosonic modes and let \hat{a}_j and \hat{a}_j^\dagger be the annihilation and creation operators associated with the j^{th} mode. Position and momentum quadrature operators are defined as $\hat{q}_j \equiv (\hat{a}_j^\dagger + \hat{a}_j)/\sqrt{2}$ and $\hat{p}_j \equiv i(\hat{a}_j^\dagger - \hat{a}_j)/\sqrt{2}$. These quadrature operators can be concisely represented by $\hat{\mathbf{x}} = (\hat{q}_1, \hat{p}_1, \dots, \hat{q}_N, \hat{p}_N)^T$.

Gaussian states are fully characterized by their first two mo-

ments $\bar{\mathbf{x}}_i \equiv \langle \hat{\mathbf{x}}_i \rangle_{\hat{\rho}}$ and $\mathbf{V}_{ij} \equiv \langle \{\hat{\mathbf{x}}_i - \bar{\mathbf{x}}_i, \hat{\mathbf{x}}_j - \bar{\mathbf{x}}_j\} / 2 \rangle_{\hat{\rho}}$ where $\langle \hat{A} \rangle_{\hat{\rho}} \equiv \text{Tr}[\hat{A}\hat{\rho}]$. (We refer the readers to Refs. [30, 31] for more detailed definition of Gaussian states.) A single-mode thermal state $\hat{\tau}(\bar{n}) \equiv \sum_{n=0}^{\infty} \frac{\bar{n}^n}{(\bar{n}+1)^{n+1}} |n\rangle\langle n|$ is a Gaussian state and is characterized by $\bar{\mathbf{x}} = \mathbf{0}$ and $\mathbf{V} = (\bar{n} + \frac{1}{2})\mathbf{I}_2$ where \mathbf{I}_2 is the 2×2 identity matrix and \bar{n} is the average number of thermal excitations.

Let $\hat{B}_{ab}(\eta)$ be the beam splitter operation acting on modes a and b with transmissivity $\eta \in [0, 1]$. Then, the Gaussian thermal loss channel with transmissivity η (or loss probability $\gamma = 1 - \eta$) and average environmental thermal photon number \bar{n}_{th} is defined as $\mathcal{N}[\eta, \bar{n}_{\text{th}}](\hat{\rho}_a) \equiv \text{Tr}_b[\hat{B}_{ab}(\eta)(\hat{\rho}_a \otimes \hat{\tau}_b(\bar{n}_{\text{th}}))\hat{B}_{ab}^\dagger(\eta)]$. Under the Gaussian thermal loss channel $\mathcal{N}[\eta, \bar{n}_{\text{th}}]$, a Gaussian input state $\hat{\rho}_G(\bar{\mathbf{x}}, \mathbf{V})$ is transformed into another Gaussian state with $\bar{\mathbf{x}}' = \mathbf{T}\bar{\mathbf{x}}$ and $\mathbf{V}' = \mathbf{T}\mathbf{V}\mathbf{T}^T + \mathbf{N}$ where

$$\mathbf{T} = \sqrt{\eta}\mathbf{I}_2 \text{ and } \mathbf{N} = (1 - \eta)(\bar{n}_{\text{th}} + \frac{1}{2})\mathbf{I}_2. \quad (1)$$

Thus, the Gaussian thermal loss channel $\mathcal{N}[\eta, \bar{n}_{\text{th}}]$ contracts the mean quadrature by a factor of $\sqrt{\eta}$ and adds a noise \mathbf{N} to the covariance matrix.

Coherent information and quantum capacity—Let us now consider transmission of quantum information from Alice to Bob through a noisy quantum channel \mathcal{N} . One way for Alice to reliably send a quantum state to Bob despite the channel noise is to use quantum error correction, i.e., Alice encodes her quantum message through an encoding map \mathcal{E} and then Bob decodes the received (corrupted) message by a decoding map \mathcal{D} , analogous to the classical communication scenario [32]. Alternatively, in the quantum realm, it is sufficient to establish noiseless non-local quantum entanglement between Alice and Bob (given that classical forward communication is free) because they can then perform the quantum teleportation protocol to transmit one quantum bit consuming one noiseless Bell pair [33].

Suppose that Alice prepares a pure local entangled state $\hat{\phi}_{A_0A} \equiv |\phi\rangle\langle\phi|_{A_0A}$ and sends a part of it (A) to Bob through a noisy channel $\mathcal{N}_{A \rightarrow B}$. Alice and Bob then obtain an approximate mixed entangled state $\hat{\sigma}_{A_0B} \equiv (\text{id}_{A_0} \otimes \mathcal{N}_{A \rightarrow B})(\hat{\phi}_{A_0A})$. Moreover, they can repeat this procedure n times to get n copies of $\hat{\sigma}_{A_0B}$. Note that there exists a one-way entanglement distillation scheme (assisted only by forward classical communication) converting n copies of $\hat{\sigma}_{A_0B}$ into $nI(A_0)B)_{\hat{\sigma}}$ copies of noiseless Bell pair in the $n \rightarrow \infty$ limit [3, 34], where $I(A)B)_{\hat{\sigma}} \equiv S(\hat{\sigma}_B) - S(\hat{\sigma}_{A_0B})$ is the coherent information of the state $\hat{\sigma}_{A_0B}$. Here, $\hat{\sigma}_B = \text{Tr}_{A_0}[\hat{\sigma}_{A_0B}]$ and $\hat{S}(\hat{\rho}) \equiv -\text{Tr}[\hat{\rho} \log_2 \hat{\rho}]$ is the quantum von Neumann entropy of a state $\hat{\rho}$. Thus, by optimizing the input state $\hat{\phi}_{A_0A}$, Alice and Bob can distill

$$Q(\mathcal{N}) \equiv \max_{\hat{\phi}_{A_0A}} I_c(\mathcal{N}_{A \rightarrow B}, \hat{\phi}_{A_0A}) \equiv \max_{\hat{\phi}_{A_0A}} I(A)B)_{\hat{\sigma}} \quad (2)$$

noiseless Bell pairs per channel use, where $Q(\mathcal{N})$ is the one-shot coherent information of the channel \mathcal{N} . Due to the quan-

tum teleportation protocol, this implies that a quantum communication rate $Q(\mathcal{N})$ (qubits per channel use) is achievable.

Interestingly, coherent information of quantum channels can be strictly superadditive, i.e., $Q(\mathcal{N} \otimes \mathcal{M}) > Q(\mathcal{N}) + Q(\mathcal{M})$ [12–17]. Thus, it may be beneficial to send a correlated input state $|\phi\rangle_{A_0A_1 \dots A_N}$ collectively to N channels to achieve a quantum communication rate $\frac{1}{N}Q(\mathcal{N}^{\otimes N})$. It then follows that the regularized coherent information is achievable:

$$\begin{aligned} Q_{\text{reg}}(\mathcal{N}) &\equiv \lim_{N \rightarrow \infty} \frac{1}{N} Q(\mathcal{N}_{A_1^N \rightarrow B_1^N}^{\otimes N}) \\ &= \lim_{N \rightarrow \infty} \frac{1}{N} \max_{\hat{\phi}_{A_0A_1^N}} I_c(\mathcal{N}_{A_1^N \rightarrow B_1^N}^{\otimes N}, \hat{\phi}_{A_0A_1^N}), \end{aligned} \quad (3)$$

where A_1^N and B_1^N represent $A_1 \dots A_N$ and $B_1 \dots B_N$, respectively. Combining this with the converse bound of the quantum capacity [35, 36] (and the equivalence between one-way entanglement distillation and quantum error correction [3]), one can establish that the quantum capacity of a channel \mathcal{N} equals the channel's regularized coherent information.

The best known lower bound of the quantum capacity of the Gaussian thermal loss channel $\mathcal{N}[\eta, \bar{n}_{\text{th}}]$ (subject to an input energy constraint $\text{Tr}[\hat{\phi}_{A_1^N} \hat{n}_{A_k}] \leq \bar{n}$ for all $k \in \{1, \dots, N\}$) is the one-shot coherent information with respect to the two-mode squeezed vacuum state $|\tau\rangle_{A_0A} = \hat{S}_{A_0A}(G)|0\rangle_{A_0}|0\rangle_A$ with a gain $G = \bar{n} + 1$, or in the channel's perspective, a single-mode thermal state $\hat{\tau}_A \equiv \text{Tr}_{A_0}[|\tau\rangle\langle\tau|_{A_0A}] = \hat{\tau}(\bar{n})$ [18]:

$$Q_{\text{reg}}^{n \leq \bar{n}}(\mathcal{N}[\eta, \bar{n}_{\text{th}}]) \geq \max[0, f(\eta, \bar{n}_{\text{th}}, \bar{n})], \quad (4)$$

where $f(\eta, \bar{n}_{\text{th}}, \bar{n})$ is defined as

$$\begin{aligned} f(\eta, \bar{n}_{\text{th}}, \bar{n}) &\equiv g(\eta\bar{n} + (1 - \eta)\bar{n}_{\text{th}}) \\ &\quad - g\left(\frac{D + (1 - \eta)(\bar{n} - \bar{n}_{\text{th}}) - 1}{2}\right) \\ &\quad - g\left(\frac{D - (1 - \eta)(\bar{n} - \bar{n}_{\text{th}}) - 1}{2}\right). \end{aligned} \quad (5)$$

Here, $D \equiv \sqrt{((1 + \eta)\bar{n} + (1 - \eta)\bar{n}_{\text{th}} + 1)^2 - 4\eta\bar{n}(\bar{n} + 1)}$ and $g(x) \equiv (x + 1) \log_2(x + 1) - x \log_2 x$ is the entropy of a thermal state $\hat{\tau}(x)$. It is an interesting open question whether this lower bound indeed equals the true quantum capacity for $\bar{n}_{\text{th}} > 0$. Here, we give a negative answer to this question by establishing a lower bound strictly larger than the one in Eq. (5) in the high loss probability and low \bar{n} regime.

Correlated thermal states—Recall that the uncorrelated N -mode thermal state $\hat{\tau}^{(N)}(\bar{n}) \equiv (\hat{\tau}(\bar{n}))^{\otimes N}$ can be generated by applying two-mode squeezing operations $\hat{S}(G)$ to modes A_k and A'_k with $k \in \{1, \dots, N\}$ and $G = \bar{n} + 1$ (see Fig. 1 (a)). To introduce correlation between different modes we start by applying fewer two-mode squeezing operations to modes A_k and A'_k with $k \in \{1, \dots, M\}$ ($M \leq N$) but with a larger gain $G_{M,N} = (N/M)\bar{n} + 1$. Thus, only the first M modes A_1, \dots, A_M are thermally populated where each mode has on

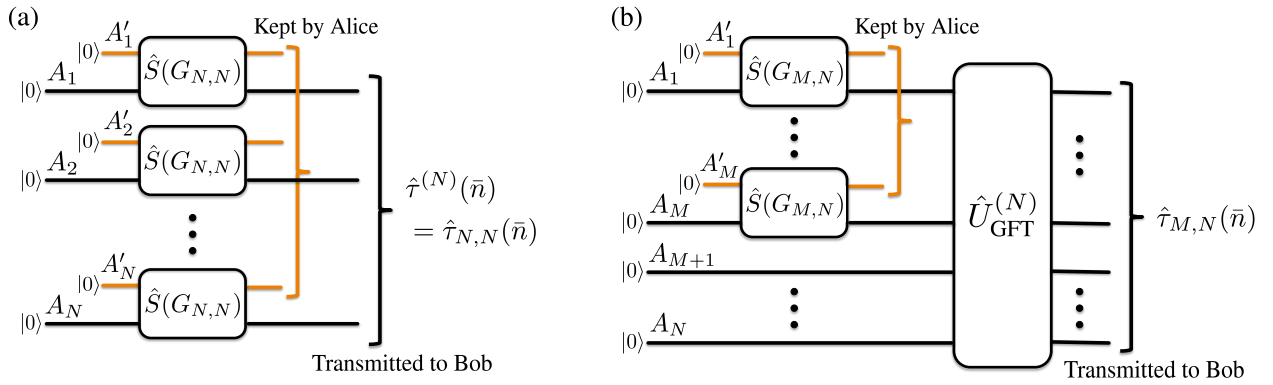


FIG. 1: Explicit Gaussian quantum circuits for the preparation of (a) uncorrelated and (b) correlated N -mode thermal states. $\hat{S}(G)$ is the two-mode squeezing unitary operation and $G_{M,N}$ is given by $G_{M,N} = (N/M)\bar{n} + 1$.

average $(N/M)\bar{n}$ photons. These excessive photons are distributed uniformly over all N modes by the Gaussian Fourier transformation $\hat{U}_{\text{GFT}}^{(N)}$:

$$\hat{U}_{\text{GFT}}^{(N)}: \hat{a}_j \rightarrow \frac{1}{\sqrt{N}} \sum_{k=1}^N e^{i\frac{2\pi}{N}(j-1)(k-1)} \hat{a}_k \quad (6)$$

for $j \in \{1, \dots, N\}$. This procedure yields a correlated N -mode thermal state, which we define as $\hat{\tau}_{M,N}(\bar{n})$, where each mode has on average \bar{n} photons (see Fig. 1 (b)). To see that these thermal states are correlated, let us for example take $M = 1$ and $N > 1$ and consider $\hat{\tau}_{1,N}(\bar{n})$. The covariance matrix of $\hat{\tau}_{1,N}(\bar{n})$ is given by

$$\mathbf{V}_{1,N}(\bar{n}) \equiv \begin{bmatrix} (\bar{n} + \frac{1}{2})\mathbf{I}_2 & \bar{n}\mathbf{I}_2 & \cdots & \bar{n}\mathbf{I}_2 \\ \bar{n}\mathbf{I}_2 & (\bar{n} + \frac{1}{2})\mathbf{I}_2 & \cdots & \bar{n}\mathbf{I}_2 \\ \vdots & \vdots & \ddots & \vdots \\ \bar{n}\mathbf{I}_2 & \bar{n}\mathbf{I}_2 & \cdots & (\bar{n} + \frac{1}{2})\mathbf{I}_2 \end{bmatrix}, \quad (7)$$

and all N modes are mutually correlated as can be seen from the non-zero off-diagonal covariance elements.

We remark that these correlated thermal states can be efficiently generated: Applying the standard fast Fourier transform (FFT) technique [37] (which is based on the divide-and-conquer idea), one can decompose the Gaussian Fourier transformation $\hat{U}_{\text{GFT}}^{(N)}$ into $\mathcal{O}(N \log N)$ single-mode phase rotations and two-mode beam splitter interactions, as opposed to the $\mathcal{O}(N^2)$ scaling for a generic case. Alternatively, exploiting the fact that operations in each divided branch can be executed in parallel, one can implement the N -mode Gaussian Fourier transformation in circuit depth $\mathcal{O}((\log N)^2)$ containing $\mathcal{O}(N(\log N)^2)$ single-mode and two-mode Gaussian rotations (see the supplement for more details).

Main result—Using these correlated thermal states, we establish the following theorem:

Theorem 1. Let $Q_{\text{reg}}^{n \leq \bar{n}}(\mathcal{N}[\eta, \bar{n}_{\text{th}}])$ be the quantum capacity of the Gaussian thermal loss channel $\mathcal{N}[\eta, \bar{n}_{\text{th}}]$ subject to an average photon number constraint ($\leq \bar{n}$) in each input mode.

Then, we have

$$Q_{\text{reg}}^{n \leq \bar{n}}(\mathcal{N}[\eta, \bar{n}_{\text{th}}]) \geq \max[0, F(\eta, \bar{n}_{\text{th}}, \bar{n})], \quad (8)$$

where $F(\eta, \bar{n}_{\text{th}}, \bar{n})$ is defined as

$$F(\eta, \bar{n}_{\text{th}}, \bar{n}) \equiv \max_{0 < x \leq 1} x f\left(\eta, \bar{n}_{\text{th}}, \frac{\bar{n}}{x}\right). \quad (9)$$

Note that $F(\eta, \bar{n}_{\text{th}}, \bar{n}) \geq f(\eta, \bar{n}_{\text{th}}, \bar{n})$ since $f(\eta, \bar{n}_{\text{th}}, \bar{n})$ can be realized by plugging in $x = 1$ to the objective function.

Sketch of the proof. We prove that the correlated N -mode thermal state $\hat{\tau}_{M,N}(\bar{n})$ yields an achievable rate $\frac{M}{N} f(\eta, \bar{n}_{\text{th}}, \frac{N}{M}\bar{n})$ by computing its coherent information per channel use (see the supplement for more details). Thus, the rate $F_x(\eta, \bar{n}_{\text{th}}, \bar{n}) \equiv x f(\eta, \bar{n}_{\text{th}}, \bar{n}/x)$ is achievable for any rational number $0 < x = \frac{M}{N} \leq 1$. Since the set of rational numbers is a dense subset of the set of real numbers, $F_x(\eta, \bar{n}_{\text{th}}, \bar{n})$ is achievable for any real $x \in (0, 1]$ and the theorem follows. ■

In Fig. 2 (a), we plot the achievable rates of the single-mode thermal states and correlated multi-mode thermal states for the Gaussian thermal loss channel $\mathcal{N}[\eta, \bar{n}_{\text{th}} = 1]$, subject to an average photon number constraint $\bar{n} \leq 1$ in each mode. When the loss probability is low (i.e., $\gamma \leq 0.1775$), a single-mode thermal state $\hat{\tau}(\bar{n})$ yields the largest coherent information. However, when the loss probability is high ($\gamma \geq 0.1775$), there exists a correlated multi-mode thermal state $\hat{\tau}_{M,N}(\bar{n})$ that outperforms the single-mode thermal state for some $N \geq 2$ and $M < N$. Thus, we established a larger lower bound of the Gaussian thermal loss channel capacity than the previous bound [18]. In Fig. 2 (b), we plot the optimal value of M/N as a function of γ that allows such a higher communication rate.

We remark that such superior performance of the correlated multi-mode thermal states becomes marginal as the energy constraint is loosened (i.e., $\bar{n} \rightarrow \infty$). To see this more explicitly, we plot in Fig. 3 the achievable rates of the single-mode and correlated multi-mode thermal states as a function

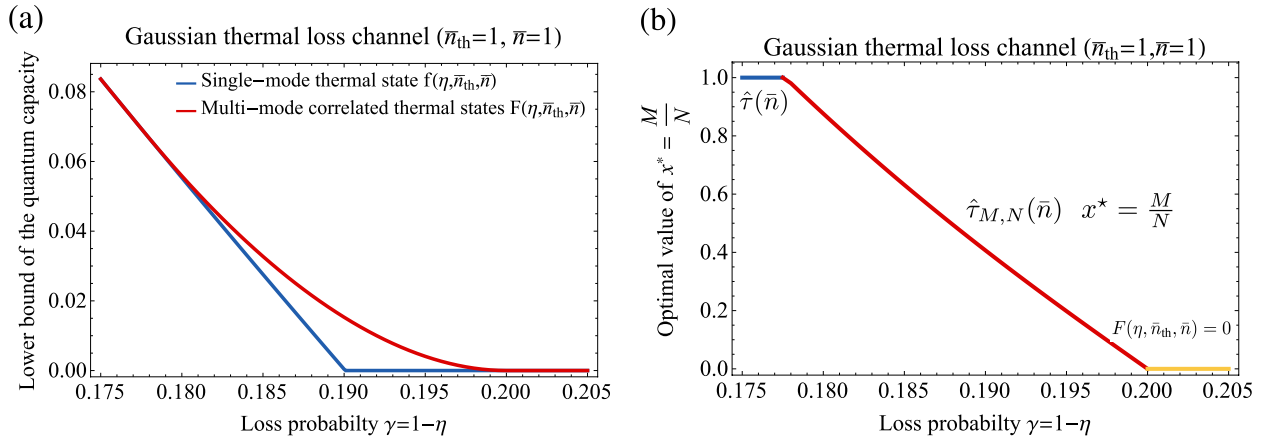


FIG. 2: (a) Maximum achievable rates of the single-mode thermal state $\hat{\tau}(\bar{n})$ (blue, Eq. (5)) and the correlated thermal states $\hat{\tau}_{M,N}(\bar{n})$ (red, Eq. (9)) with $\bar{n} = 1$ for the Gaussian thermal loss channel $\mathcal{N}[\eta, \bar{n}_{\text{th}} = 1]$. For the correlated thermal states, the achievable rate was optimized by taking $M/N = x^* = \text{argmax}_{0 < x \leq 1} x f(\eta, \bar{n}_{\text{th}}, \bar{n}/x)$. (b) The optimal value of $x^* = M/N$ at each γ , color-coded by the type of optimizer (single-mode thermal states, correlated multi-mode thermal states), that allows the maximum achievable rate. We set $x^* = M/N = 0$ when all the states we consider yield vanishing achievable rates (yellow).

of \bar{n} for the Gaussian thermal loss channel $\mathcal{N}[\eta, \bar{n}_{\text{th}}]$ with $\eta = 1 - \gamma = 0.81$ and $\bar{n}_{\text{th}} = 1$. As can be seen from Fig. 3, for a given $\mathcal{N}[\eta, \bar{n}_{\text{th}}]$, the correlated multi-mode thermal states outperform the single-mode thermal states only when \bar{n} is smaller than a threshold value $\bar{n}^*(\eta, \bar{n}_{\text{th}})$ (e.g., $\bar{n}^*(0.81, 1) = 2.458$). We observe that $\bar{n}^*(\eta, \bar{n}_{\text{th}})$ is a decreasing function of $\gamma = 1 - \eta$ and \bar{n}_{th} and thus the effects of correlation are strong in the high loss probability and high thermal noise regime. We also observe that there exists a range of γ where correlated multi-mode thermal states outperform single-mode thermal states for any given finite input average photon number $\bar{n} < \infty$. However, such a region becomes narrower as \bar{n} increases and eventually shrinks to a point as $\bar{n} \rightarrow \infty$.

Finally, we remark that the non-trivial advantage of the correlated multi-mode thermal states comes from the convexity

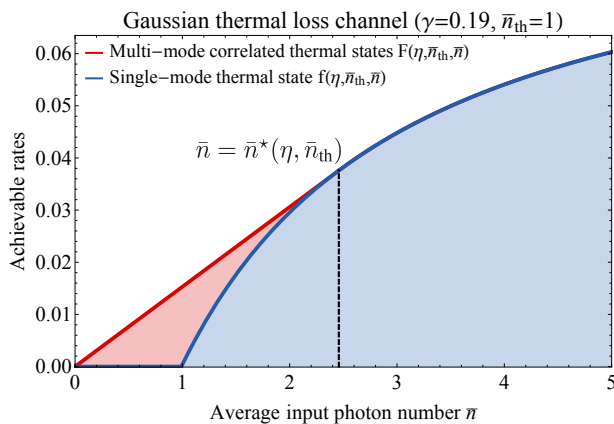


FIG. 3: Achievable rates of the single-mode and correlated multi-mode thermal states as a function of \bar{n} .

of the function $f(\eta, \bar{n}_{\text{th}}, \bar{n})$ in \bar{n} : Define $A_{\eta, \bar{n}_{\text{th}}}^{(1)} \equiv \{(\bar{n}, R) | \bar{n} \geq 0 \text{ and } R = f(\eta, \bar{n}_{\text{th}}, \bar{n})\}$. Then, consider the convex hull of $A_{\eta, \bar{n}_{\text{th}}}^{(1)}$, i.e., $A_{\eta, \bar{n}_{\text{th}}}^{(\infty)} \equiv \{(\sum_i \lambda_i \bar{n}_i, \sum_i \lambda_i f(\eta, \bar{n}_{\text{th}}, \bar{n}_i)) | \lambda_i \in [0, 1] \text{ and } \sum_i \lambda_i = 1\}$. Using a more general version of Theorem 1, one can show that $A_{\eta, \bar{n}_{\text{th}}}^{(\infty)}$ is in the achievable region (see the supplement for more details). Due to the convexity of $f(\eta, \bar{n}_{\text{th}}, \bar{n})$, $A_{\eta, \bar{n}_{\text{th}}}^{(\infty)}$ properly contains $A_{\eta, \bar{n}_{\text{th}}}^{(1)}$, as indicated by the red region in Fig. 3. This explains why the correlated multi-mode thermal states outperform the single-mode thermal states in some parameter regime.

Discussion—Recall that the improved achievable rate established in Eq. (9) (see also Fig. 2) is based on the existence of an entanglement distillation scheme in which n copies of $\hat{\sigma}_{AB}$ can be distilled into $nI(A)B)_{\hat{\sigma}}$ copies of the perfect Bell pairs [34]. However, the proof of existence is based on a random coding argument and thus is not constructive. In addition, although a correlated thermal state $\hat{\tau}_{M,N}(\bar{n})$ (and its purification $|\tau_{M,N}(\bar{n})\rangle$) can be efficiently prepared using only Gaussian operations, entanglement distillation of the noisy output entangled state $\mathcal{N}[\eta, \bar{n}_{\text{th}}]^{\otimes N}(|\tau_{M,N}(\bar{n})\rangle\langle\tau_{M,N}(\bar{n})|)$ cannot be performed by using only Gaussian operations due to a no-go theorem established in Ref. [38]. Thus, it will be an interesting research avenue to search for an efficient entanglement distillation scheme (e.g., with few non-Gaussian operations) that achieves the communication rates established in this letter. Similarly, it will also be interesting to look for an explicit quantum error-correcting codes (such as GKP codes [23, 39, 40]) and an efficient decoding strategy that achieves (or improves) the rates established here.

We emphasize that we do not claim superadditivity of Gaussian thermal loss channels because it is not proven that the single-mode thermal state $\hat{\tau}(\bar{n})$ is an optimal input state for the one-shot coherent information of Gaussian thermal loss channels: It is still possible that there may exist a single-

mode input state that outperforms the correlated multi-mode thermal states.

Conclusion—We introduced correlated multi-mode thermal states and showed that they can provide larger achievable quantum communication rate for Gaussian thermal loss channels than the single-mode thermal state. Thus, we established a lower bound of the Gaussian thermal loss channel capacity, which is larger than the best known lower bound. We also constructed explicit Gaussian quantum circuits which can efficiently implement such correlated multi-mode thermal states.

Acknowledgment—We would like to thank Steve Girvin, Mark Wilde and Kunal Sharma for helpful discussions. We acknowledge support from the ARL-CDQI (W911NF-15-2-0067, W911NF-18-2-0237), ARO (W911NF-18-1-0020, W911NF-18-1-0212), ARO MURI (W911NF-16-1-0349), AFOSR MURI (FA9550-14-1-0052, FA9550-15-1-0015), DOE (DE-SC0019406), NSF (EFMA-1640959), and the Packard Foundation (2013-39273). K.N. acknowledges support through the Korea Foundation for Advanced Studies.

* kyungjoo.noh@yale.edu

- [1] C. H. Bennett, H. J. Bernstein, S. Popescu, and B. Schumacher, “Concentrating partial entanglement by local operations,” *Phys. Rev. A* **53**, 2046–2052 (1996).
- [2] C. H. Bennett, G. Brassard, S. Popescu, B. Schumacher, J. A. Smolin, and W. K. Wootters, “Purification of noisy entanglement and faithful teleportation via noisy channels,” *Phys. Rev. Lett.* **76**, 722–725 (1996).
- [3] C. H. Bennett, D. P. DiVincenzo, J. A. Smolin, and W. K. Wootters, “Mixed-state entanglement and quantum error correction,” *Phys. Rev. A* **54**, 3824–3851 (1996).
- [4] M. M. Wilde, *Quantum Information Theory* (Cambridge University Press, 2013).
- [5] B. Schumacher and M. A. Nielsen, “Quantum data processing and error correction,” *Phys. Rev. A* **54**, 2629–2635 (1996).
- [6] S. Lloyd, “Capacity of the noisy quantum channel,” *Phys. Rev. A* **55**, 1613–1622 (1997).
- [7] I. Devetak, “The private classical capacity and quantum capacity of a quantum channel,” *IEEE Transactions on Information Theory* **51**, 44–55 (2005).
- [8] M. M. Wilde and H. Qi, “Energy-constrained private and quantum capacities of quantum channels,” *ArXiv e-prints*, arXiv:1609.01997 (2016), arXiv:1609.01997 [quant-ph].
- [9] I. Devetak and P. W. Shor, “The capacity of a quantum channel for simultaneous transmission of classical and quantum information,” *Communications in Mathematical Physics* **256**, 287–303 (2005).
- [10] J. Yard, P. Hayden, and I. Devetak, “Capacity theorems for quantum multiple-access channels: classical-quantum and quantum-quantum capacity regions,” *IEEE Transactions on Information Theory* **54**, 3091–3113 (2008).
- [11] F. Caruso and V. Giovannetti, “Degradability of bosonic Gaussian channels,” *Phys. Rev. A* **74**, 062307 (2006).
- [12] D. P. DiVincenzo, P. W. Shor, and J. A. Smolin, “Quantum-channel capacity of very noisy channels,” *Phys. Rev. A* **57**, 830–839 (1998).
- [13] G. Smith and J. Yard, “Quantum communication with zero-capacity channels,” *Science* **321**, 1812–1815 (2008).
- [14] G. Smith, J. A. Smolin, and J. Yard, “Quantum communication with Gaussian channels of zero quantum capacity,” *Nature Photonics* **5**, 624–627 (2011).
- [15] T. Cubitt, D. Elkouss, W. Matthews, M. Ozols, D. Pérez-García, and S. Strelchuk, “Unbounded number of channel uses may be required to detect quantum capacity,” *Nature Communications* **6**, 6739 (2015).
- [16] Y. Lim and S. Lee, “Activation of the quantum capacity of gaussian channels,” *Phys. Rev. A* **98**, 012326 (2018).
- [17] F. Leditzky, D. Leung, and G. Smith, “Dephasure channel and superadditivity of coherent information,” *Phys. Rev. Lett.* **121**, 160501 (2018).
- [18] A. S. Holevo and R. F. Werner, “Evaluating capacities of bosonic Gaussian channels,” *Phys. Rev. A* **63**, 032312 (2001).
- [19] G. Smith and J. A. Smolin, “Degenerate quantum codes for pauli channels,” *Phys. Rev. Lett.* **98**, 030501 (2007).
- [20] J. Fern and K. B. Whaley, “Lower bounds on the nonzero capacity of pauli channels,” *Phys. Rev. A* **78**, 062335 (2008).
- [21] K. Sharma, M. M. Wilde, S. Adhikari, and M. Takeoka, “Bounding the energy-constrained quantum and private capacities of phase-insensitive bosonic gaussian channels,” *New Journal of Physics* **20**, 063025 (2018).
- [22] M. Rosati, A. Mari, and V. Giovannetti, “Narrow bounds for the quantum capacity of thermal attenuators,” *Nature Communications* **9**, 4339 (2018).
- [23] K. Noh, V. V. Albert, and L. Jiang, “Improved quantum capacity bounds of Gaussian loss channels and achievable rates with Gottesman-Kitaev-Preskill codes,” *ArXiv e-prints*, arXiv:1801.07271 (2018), arXiv:1801.07271 [quant-ph].
- [24] D. Sutter, V. B. Scholz, A. Winter, and R. Renner, “Approximate degradable quantum channels,” *IEEE Transactions on Information Theory* **63**, 7832–7844 (2017).
- [25] F. Leditzky, D. Leung, and G. Smith, “Quantum and private capacities of low-noise channels,” *Phys. Rev. Lett.* **120**, 160503 (2018).
- [26] M. M. Wolf, D. Pérez-García, and G. Giedke, “Quantum capacities of bosonic channels,” *Phys. Rev. Lett.* **98**, 130501 (2007).
- [27] M. M. Wilde, P. Hayden, and S. Guha, “Quantum trade-off coding for bosonic communication,” *Phys. Rev. A* **86**, 062306 (2012).
- [28] F. Caruso, V. Giovannetti, and A. S. Holevo, “One-mode bosonic Gaussian channels: a full weak-degradability classification,” *New Journal of Physics* **8**, 310 (2006).
- [29] A. S. Holevo, “One-mode quantum Gaussian channels: Structure and quantum capacity,” *Problems of Information Transmission* **43**, 1–11 (2007).
- [30] C. Weedbrook, S. Pirandola, R. García-Patrón, N. J. Cerf, T. C. Ralph, J. H. Shapiro, and S. Lloyd, “Gaussian quantum information,” *Rev. Mod. Phys.* **84**, 621–669 (2012).
- [31] A. Serafini, *Quantum Continuous Variables* (CRC Press, 2017).
- [32] Shannon C. E., “A mathematical theory of communication,” *Bell System Technical Journal* **27**, 379–423, <https://onlinelibrary.wiley.com/doi/pdf/10.1002/j.1538-7305.1948.tb01338.x>.
- [33] C. H. Bennett, G. Brassard, C. Crépeau, R. Jozsa, A. Peres, and W. K. Wootters, “Teleporting an unknown quantum state via dual classical and Einstein-Podolsky-Rosen channels,” *Phys. Rev. Lett.* **70**, 1895–1899 (1993).
- [34] I. Devetak and A. Winter, “Distillation of secret key and entanglement from quantum states,” *Proceedings of the Royal Society of London A: Mathematical, Physical and Engineering Sciences* **461**, 207–235 (2005), <http://rspa.royalsocietypublishing.org/content/461/2053/207.full.pdf>.
- [35] H. Barnum, M. A. Nielsen, and B. Schumacher, “Information

- transmission through a noisy quantum channel,” Phys. Rev. A **57**, 4153–4175 (1998).
- [36] H. Barnum, E. Knill, and M. A. Nielsen, “On quantum fidelities and channel capacities,” IEEE Transactions on Information Theory **46**, 1317–1329 (2000).
- [37] J. W. Cooley and J. W. Tukey, “An algorithm for the machine calculation of complex fourier series,” Mathematics of Computation **19**, 297–301 (1965).

- [38] J. Eisert, S. Scheel, and M. B. Plenio, “Distilling Gaussian states with Gaussian operations is impossible,” Phys. Rev. Lett. **89**, 137903 (2002).
- [39] D. Gottesman and J. Preskill, “Secure quantum key distribution using squeezed states,” Phys. Rev. A **63**, 022309 (2001).
- [40] J. Harrington and J. Preskill, “Achievable rates for the Gaussian quantum channel,” Phys. Rev. A **64**, 062301 (2001).

SUPPLEMENTAL MATERIAL

In the supplemental material, we provide a detailed proof of Theorem 1 present a more general version of Theorem 1. We also prove that the N -mode Gaussian Fourier transformation can be implemented in circuit depth $\mathcal{O}((\log N)^2)$ using $\mathcal{O}(N(\log N)^2)$ single-mode and two-mode Gaussian rotations.

DETAILED PROOF OF THEOREM 1

Consider a correlated thermal state $\hat{\tau}_{M,N}(\bar{n})$ and its purification $|\tau_{M,N}(\bar{n})\rangle_{A_0 A_1^N}$, where $A_1^N \equiv A_1 \cdots A_N$. Recall that the coherent information per channel use is an achievable rate:

$$R_{M,N}(\eta, \bar{n}_{\text{th}}, \bar{n}) \equiv \frac{1}{N} I_c(\mathcal{N}_{A_1^N \rightarrow B_1^N}^{\otimes N}, |\tau_{M,N}(\bar{n})\rangle \langle \tau_{M,N}(\bar{n})|_{A_0 A_1^N}). \quad (\text{S1})$$

Exploiting the notion of complementary channel, one can rewrite Eq. (S1) solely in terms of the mixed input state $\hat{\tau}_{M,N}(\bar{n})$:

$$R_{M,N}(\eta, \bar{n}_{\text{th}}, \bar{n}) = \frac{1}{N} \left[S\left(\mathcal{N}[\eta, \bar{n}_{\text{th}}]^{\otimes N}(\hat{\tau}_{M,N}(\bar{n}))\right) - S\left(\mathcal{N}^c[\eta, \bar{n}_{\text{th}}]^{\otimes N}(\hat{\tau}_{M,N}(\bar{n}))\right) \right], \quad (\text{S2})$$

where $\mathcal{N}^c[\eta, \bar{n}_{\text{th}}]$ is a complementary channel of the Gaussian thermal loss channel $\mathcal{N}[\eta, \bar{n}_{\text{th}}]$ (see, e.g., Ref. [4]). $\mathcal{N}^c[\eta, \bar{n}_{\text{th}}]$ can be chosen to be a Gaussian channel transforming an input Gaussian state $\hat{\rho}_G(\bar{x}, \mathbf{V})$ into another Gaussian state $\hat{\rho}_G(\bar{x}', \mathbf{V}')$ with $\bar{x}' = \mathbf{T}_c \bar{x}$ and $\mathbf{V}' = \mathbf{T}_c \mathbf{V} \mathbf{T}_c^T + \mathbf{N}_c$, where \mathbf{T}_c and \mathbf{N}_c are given by

$$\mathbf{T}_c = \begin{bmatrix} -\sqrt{1-\eta} \mathbf{I}_2 \\ \mathbf{0} \end{bmatrix}, \quad \text{and} \quad \mathbf{N}_c = \begin{bmatrix} \eta(\bar{n}_{\text{th}} + \frac{1}{2}) \mathbf{I}_2 & \sqrt{\eta \bar{n}_{\text{th}}(\bar{n}_{\text{th}} + 1)} \mathbf{Z}_2 \\ \sqrt{\eta \bar{n}_{\text{th}}(\bar{n}_{\text{th}} + 1)} \mathbf{Z}_2 & (\bar{n}_{\text{th}} + \frac{1}{2}) \mathbf{I}_2 \end{bmatrix}, \quad (\text{S3})$$

and $\mathbf{Z}_2 \equiv \text{diag}(1, -1)$. Extending the channel specifications of $\mathcal{N}[\eta, \bar{n}_{\text{th}}]$ and $\mathcal{N}^c[\eta, \bar{n}_{\text{th}}]$ in Eqs. (1),(S3) to the N -mode case, we find

$$\begin{aligned} \mathbf{T}^{(N)} &= \sqrt{\eta} \mathbf{I}_{2N}, & \mathbf{N}^{(N)} &= (1-\eta) \left(\bar{n}_{\text{th}} + \frac{1}{2} \right) \mathbf{I}_{2N}, \\ \mathbf{T}_c^{(N)} &= \begin{bmatrix} -\sqrt{1-\eta} \mathbf{I}_{2N} \\ \mathbf{0} \end{bmatrix}, & \mathbf{N}_c^{(N)} &= \begin{bmatrix} \eta(\bar{n}_{\text{th}} + \frac{1}{2}) \mathbf{I}_{2N} & \sqrt{\eta \bar{n}_{\text{th}}(\bar{n}_{\text{th}} + 1)} \mathbf{Z}_{2N} \\ \sqrt{\eta \bar{n}_{\text{th}}(\bar{n}_{\text{th}} + 1)} \mathbf{Z}_{2N} & (\bar{n}_{\text{th}} + \frac{1}{2}) \mathbf{I}_{2N} \end{bmatrix}, \end{aligned} \quad (\text{S4})$$

where $\mathbf{Z}_{2N} \equiv \bigoplus_{k=1}^N \mathbf{Z}_2 = \text{diag}(1, -1, \dots, 1, -1)$.

Recall the defining quantum circuit of the correlated thermal state $\hat{\tau}_{M,N}(\bar{n})$ in Fig. 1. The correlated thermal state $\hat{\tau}_{M,N}(\bar{n})$ is given by

$$\hat{\tau}_{M,N}(\bar{n}) = \mathcal{U}_{\text{GFT}}^{(N)} \left(\hat{\tau} \left(\frac{N}{M} \bar{n} \right)^{\otimes M} \otimes |0\rangle\langle 0|^{\otimes N-M} \right), \quad (\text{S5})$$

where $\mathcal{U}_{\text{GFT}}^{(N)}(\hat{\rho}) \equiv \hat{U}_{\text{GFT}}^{(N)} \hat{\rho} (\hat{U}_{\text{GFT}}^{(N)})^\dagger$. Note that the symplectic transformation matrix $\mathbf{S}_{\text{GFT}}^{(N)}$ associated with the N -mode Gaussian

transformation $\hat{U}_{\text{GFT}}^{(N)}$ is given by

$$\mathbf{S}_{\text{GFT}}^{(N)} = \frac{1}{\sqrt{N}} \begin{bmatrix} \mathbf{R}(0) & \mathbf{R}(0) & \cdots & \mathbf{R}(0) \\ \mathbf{R}(0) & \mathbf{R}(\frac{2\pi}{N}) & \cdots & \mathbf{R}(\frac{2\pi}{N}(N-1)) \\ \vdots & \vdots & \ddots & \vdots \\ \mathbf{R}(0) & \mathbf{R}(\frac{2\pi}{N}(N-1)) & \cdots & \mathbf{R}(\frac{2\pi}{N}(N-1)^2) \end{bmatrix}, \text{ where } \mathbf{R}(\theta) \equiv \begin{bmatrix} \cos \theta & -\sin \theta \\ \sin \theta & \cos \theta \end{bmatrix}. \quad (\text{S6})$$

Since $\mathbf{S}_{\text{GFT}}^{(N)}$ is an orthogonal matrix, i.e., $\mathbf{S}_{\text{GFT}}^{(N)}(\mathbf{S}_{\text{GFT}}^{(N)})^T = (\mathbf{S}_{\text{GFT}}^{(N)})^T \mathbf{S}_{\text{GFT}}^{(N)} = \mathbf{I}$, one can immediately see that

$$\mathcal{N}[\eta, \bar{n}_{\text{th}}]^{\otimes N} \left(\mathcal{U}_{\text{GFT}}^{(N)}(\hat{\rho}) \right) = \mathcal{U}_{\text{GFT}}^{(N)} \left(\mathcal{N}[\eta, \bar{n}_{\text{th}}]^{\otimes N}(\hat{\rho}) \right), \quad (\text{S7})$$

because $\mathbf{S}_{\text{GFT}}^{(N)} \mathbf{T}^{(N)} = \mathbf{T}^{(N)} \mathbf{S}_{\text{GFT}}^{(N)}$ and $\mathbf{S}_{\text{GFT}}^{(N)} \mathbf{N}^{(N)} (\mathbf{S}_{\text{GFT}}^{(N)})^T = \mathbf{N}^{(N)}$. Similarly, we also have

$$\mathcal{N}^c[\eta, \bar{n}_{\text{th}}]^{\otimes N} \left(\mathcal{U}_{\text{GFT}}^{(N)}(\hat{\rho}) \right) = \left(\mathcal{U}_{\text{GFT}}^{(N)} \otimes (\mathcal{U}_{\text{GFT}}^{(N)})^{-1} \right) \left(\mathcal{N}^c[\eta, \bar{n}_{\text{th}}]^{\otimes N}(\hat{\rho}) \right), \quad (\text{S8})$$

because $(\mathbf{S}_{\text{GFT}}^{(N)} \oplus (\mathbf{S}_{\text{GFT}}^{(N)})^{-1}) \mathbf{T}_c^{(N)} = \mathbf{T}_c^{(N)} \mathbf{S}_{\text{GFT}}^{(N)}$ and $(\mathbf{S}_{\text{GFT}}^{(N)} \oplus (\mathbf{S}_{\text{GFT}}^{(N)})^{-1}) \mathbf{N}_c^{(N)} (\mathbf{S}_{\text{GFT}}^{(N)} \oplus (\mathbf{S}_{\text{GFT}}^{(N)})^{-1})^T = \mathbf{N}_c^{(N)}$. Using the fact that the von Neumann entropy is invariant under a unitary transformation, we can simplify Eq. (S2) as

$$\begin{aligned} R_{M,N}(\eta, \bar{n}_{\text{th}}, \bar{n}) &= \frac{1}{N} \left[S \left(\mathcal{N}[\eta, \bar{n}_{\text{th}}]^{\otimes N} \left(\hat{\tau} \left(\frac{N}{M} \bar{n} \right)^{\otimes M} \otimes |0\rangle\langle 0|^{\otimes N-M} \right) \right) \right. \\ &\quad \left. - S \left(\mathcal{N}^c[\eta, \bar{n}_{\text{th}}]^{\otimes N} \left(\hat{\tau} \left(\frac{N}{M} \bar{n} \right)^{\otimes M} \otimes |0\rangle\langle 0|^{\otimes N-M} \right) \right) \right] \\ &= \frac{M}{N} f \left(\eta, \bar{n}_{\text{th}}, \frac{N}{M} \bar{n} \right) + \frac{(N-M)}{N} f(\eta, \bar{n}_{\text{th}}, 0) \\ &= \frac{M}{N} f \left(\eta, \bar{n}_{\text{th}}, \frac{N}{M} \bar{n} \right). \end{aligned} \quad (\text{S9})$$

Thus, $F_x(\eta, \bar{n}_{\text{th}}, \bar{n}) \equiv x f(\eta, \bar{n}_{\text{th}}, \bar{n}/x)$ is achievable for any rational number $0 < x = \frac{M}{N} \leq 1$.

Consider an irrational number $x \in (0, 1)$ and its decimal representation: $x = [0.x_1 x_2 \cdots]_{10} = \sum_{i=1}^{\infty} x_i 10^{-i}$ where $x_i \in \{0, \dots, 9\}$. Define a sequence $(a_n)_{n \in \mathbb{N}}$ where

$$a_n \equiv (M_n, N_n), \text{ with } M_n = [x_1 \cdots x_n]_{10} = \sum_{i=1}^n x_i 10^{n-i}, \text{ and } N = 10^n. \quad (\text{S10})$$

Now, consider the associated sequence of achievable rates $(R_n)_{n \in \mathbb{N}}$ where R_n is defined as

$$R_n \equiv \frac{M_n}{N_n} f \left(\eta, \bar{n}_{\text{th}}, \frac{N_n}{M_n} \bar{n} \right). \quad (\text{S11})$$

Note that $\lim_{n \rightarrow \infty} \frac{M_n}{N_n} = x$. Since $F_{x'}(\eta, \bar{n}_{\text{th}}, \bar{n}) \equiv x' f(\eta, \bar{n}_{\text{th}}, \bar{n}/x')$ is a continuous function of x' , we have

$$\lim_{n \rightarrow \infty} R_n = \left(\lim_{n \rightarrow \infty} \frac{M_n}{N_n} \right) f \left(\eta, \bar{n}_{\text{th}}, \left(\lim_{n \rightarrow \infty} \frac{N_n}{M_n} \right) \bar{n} \right) = x f \left(\eta, \bar{n}_{\text{th}}, \left(\frac{\bar{n}}{x} \right) \right) = F_x(\eta, \bar{n}_{\text{th}}, \bar{n}). \quad (\text{S12})$$

Thus, $F_x(\eta, \bar{n}_{\text{th}}, \bar{n})$ is achievable for any real number $x \in (0, 1]$ and the theorem follows.

A MORE GENERAL VERSION OF THEOREM 1

Theorem 2. Recall the definition of $A_{\eta, \bar{n}_{\text{th}}}^{(\infty)}$:

$$A_{\eta, \bar{n}_{\text{th}}}^{(\infty)} \equiv \left\{ \left(\sum_i \lambda_i \bar{n}_i, \sum_i \lambda_i f(\eta, \bar{n}_{\text{th}}, \bar{n}_i) \right) \mid \lambda_i \in [0, 1] \text{ and } \sum_i \lambda_i = 1 \right\}. \quad (\text{S13})$$

Then, $A_{\eta, \bar{n}_{\text{th}}}^{(\infty)}$ is in the achievable region.

Proof. Let $\vec{\lambda} = (\lambda_1, \lambda_2, \dots)$ and $\vec{n} = (\bar{n}_1, \bar{n}_2, \dots)$ and consider the following type of correlated thermal state:

$$\hat{\tau}_{\vec{\lambda}, \vec{n}} \equiv \mathcal{U}_{\text{GFT}}^{(N)} \left(\bigotimes_i \hat{\tau}(\bar{n}_i)^{\otimes \lambda_i N} \right). \quad (\text{S14})$$

That is, $\hat{\tau}_{\vec{\lambda}, \vec{n}}$ is generated by applying the N -mode Gaussian Fourier transformation $\mathcal{U}_{\text{GFT}}^{(N)}$ to the uncorrelated thermal state $\bigotimes_i \hat{\tau}(\bar{n}_i)^{\otimes \lambda_i N}$ where the first $\lambda_1 N$ modes support the thermal state with an average photon number \bar{n}_1 and the next $\lambda_2 N$ modes support the thermal state with an average photon number \bar{n}_2 , and so on. Then, following the same argument used to prove Theorem 1, one can show that the achievable rate of the state $\hat{\tau}_{\vec{\lambda}, \vec{n}}$ is given by

$$R_{\vec{\lambda}, \vec{n}}(\eta, \bar{n}_{\text{th}}) = \sum_i \lambda_i f(\eta, \bar{n}_{\text{th}}, \bar{n}_i). \quad (\text{S15})$$

Note that the total average photon number of the state $\hat{\tau}_{\vec{\lambda}, \vec{n}}$ is given by $N \sum_i \lambda_i \bar{n}_i$. Since the Gaussian Fourier transformation distributes the photons uniformly over all N modes, each mode of the state $\hat{\tau}_{\vec{\lambda}, \vec{n}}$ contains on average $\sum_i \lambda_i \bar{n}_i$ photons. This then implies that $(\bar{n}, R) = (\sum_i \lambda_i \bar{n}_i, \sum_i \lambda_i f(\eta, \bar{n}_{\text{th}}, \bar{n}_i))$ is in the achievable region and the theorem follows. ■

Theorem 1 is a special case of Theorem 2 since Theorem 1 can be recovered by specializing Theorem 2 to $\vec{\lambda} = (1 - x, x)$ and $\vec{n} = (0, \frac{\bar{n}}{x})$. However, we observe that more general convex combinations considered in Theorem 2 do not yield larger achievable rates than the ones in Theorem 1 because, as can be seen from Fig. 3, the non-trivial boundary of the region $A_{\eta, \bar{n}_{\text{th}}}^{(\infty)}$ is given by the line starting from the origin that is in the first-order contact with $A_{\eta, \bar{n}_{\text{th}}}^{(1)}$ (see the bold red line in Fig. 3). This is why we only presented Theorem 1 in the main text.

EFFICIENT IMPLEMENTATION OF THE GAUSSIAN FOURIER TRANSFORMATION

Let us now consider circuit complexity of the Gaussian Fourier transformation. For simplicity, we only consider $N = 2^m$ for some $m \in \{1, 2, \dots\}$. Following the standard divide-and-conquer technique [37], we decompose a $2N$ -mode Gaussian Fourier transformation $\hat{U}_{\text{GFT}}^{(2N)}$ into two N -mode Gaussian transformations $\hat{U}_{\text{GFT}}^{(N)}$ modulo pre- and post-processing:

$$\begin{aligned} \begin{pmatrix} \hat{a}_{2k} \\ \hat{a}_{2k+1} \end{pmatrix} &\xrightarrow[\text{Perfect shuffling}]{} \begin{pmatrix} \hat{a}_k \\ \hat{a}_{N+k} \end{pmatrix} \xrightarrow[\text{N-mode GFT}]{} \frac{1}{\sqrt{N}} \begin{pmatrix} \sum_{\ell=0}^{N-1} e^{i \frac{2\pi}{N} k \ell} \hat{a}_\ell \\ \sum_{\ell=0}^{N-1} e^{i \frac{2\pi}{N} k \ell} \hat{a}_{N+\ell} \end{pmatrix} \xrightarrow[\text{Phase rotation}]{} \frac{1}{\sqrt{N}} \begin{pmatrix} \sum_{\ell=0}^{N-1} e^{i \frac{2\pi}{2N} 2k \ell} \hat{a}_\ell \\ \sum_{\ell=0}^{N-1} e^{i \frac{2\pi}{2N} (2k+1) \ell} \hat{a}_{N+\ell} \end{pmatrix} \\ &\xrightarrow[\text{Two-mode GFT}]{} \frac{1}{\sqrt{2N}} \begin{pmatrix} \sum_{\ell=0}^{N-1} e^{i \frac{2\pi}{2N} 2k \ell} (\hat{a}_\ell + \hat{a}_{N+\ell}) \\ \sum_{\ell=0}^{N-1} e^{i \frac{2\pi}{2N} (2k+1) \ell} (\hat{a}_\ell - \hat{a}_{N+\ell}) \end{pmatrix} = \frac{1}{\sqrt{2N}} \begin{pmatrix} \sum_{\ell=0}^{2N-1} e^{i \frac{2\pi}{2N} 2k \ell} \hat{a}_\ell \\ \sum_{\ell=0}^{2N-1} e^{i \frac{2\pi}{2N} (2k+1) \ell} \hat{a}_\ell \end{pmatrix}. \end{aligned} \quad (\text{S16})$$

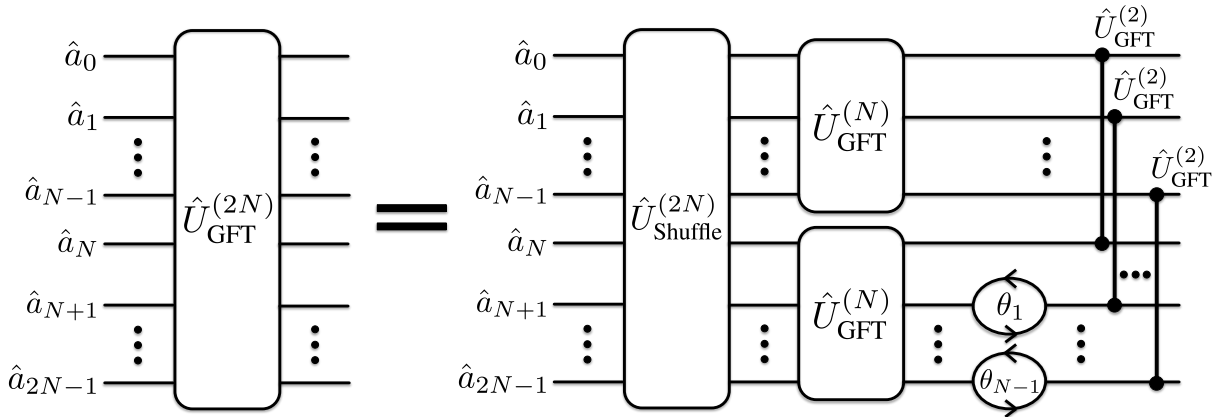


FIG. S1: Decomposition of a $2N$ -mode Gaussian Fourier transformation into a $2N$ -mode perfect shuffling ($\hat{a}_{2k} \rightarrow \hat{a}_k$, $\hat{a}_{2k+1} \rightarrow \hat{a}_{N+k}$), two N -mode Gaussian Fourier transformations, $N - 1$ phase rotations by an angle $\theta_k = \pi k/N$ on the mode $N + k$ and N two-mode Gaussian Fourier transformations on the modes k and $N + k$ for $k \in \{0, \dots, N - 1\}$.

(See Fig. S1.) Note that the $2N$ -mode perfect shuffling ($\hat{a}_{2k} \rightarrow \hat{a}_k, \hat{a}_{2k+1} \rightarrow \hat{a}_{N+k}$) can be implemented by using at most $2N$ two-mode SWAP operations ($\hat{a}_i \leftrightarrow \hat{a}_j$ and $\hat{a}_k \rightarrow \hat{a}_k$ for $k \neq i, j$), if one does not attempt to parallelize the circuit (see the discussion below). Let $\text{Op}(N)$ be the minimum total number of single-mode rotations and two-mode beam-splitter operations to implement the N -mode Gaussian Fourier transformation. Then, due to the circuit decomposition in Fig. S1, we have

$$\text{Op}(2N) \leq 2\text{Op}(N) + cN, \quad (\text{S17})$$

for some constant $c > 0$ (which can be chosen to be 4) and $N \geq 2$. Using $\text{Op}(2) = 2$ and mathematical induction, one can prove

$$\text{Op}(N) \leq cN \log_2 N = \mathcal{O}(N \log N). \quad (\text{S18})$$

Observe that many operations in Fig. S1 can be parallelized. For example, the two N -mode Gaussian Fourier transformations can be executed in parallel. Similarly, the $N - 1$ single-mode phase rotations and the N two-mode Gaussian Fourier transformations can also be implemented simultaneously. Most importantly, the $2N$ -mode perfect shuffling can be implemented in circuit depth $\log_2 N$ with $\frac{N}{2} \log_2 N$ two-mode SWAP operations: Recall that the $2N$ -mode perfect shuffling operation maps $2k$ and $2k + 1$ to $f^{(2N)}(2k) = k$ and $f^{(2N)}(2k + 1) = N + k$ respectively for $k \in \{0, \dots, N - 1\}$. Let $2N = 2^{m+1}$ and express the inputs $2k$ and $2k + 1$ in the binary representation, i.e., $2k \equiv [b_m b_{m-1} \dots b_1 0]_2$ and $2k + 1 \equiv [b_m b_{m-1} \dots b_1 1]_2$. Upon the perfect shuffling, these inputs are mapped to $k = [0 b_m b_{m-1} \dots b_1]_2$ and $N + k = [1 b_m b_{m-1} \dots b_1]_2$. Thus, the perfect shuffling shifts every bit in the binary representation to the right by one site, i.e.,

$$f^{(2N)}([b_m b_{m-1} \dots b_1 b_0]_2) = [b_0 b_m \dots b_2 b_1]_2. \quad (\text{S19})$$

Let $f_{i,j}^{(2N)}$ be a function that exchanges the bits b_i and b_j ($i > j$):

$$f_{i,j}^{(2N)}([\dots b_i \dots b_j \dots]_2) = [\dots b_j \dots b_i \dots]_2. \quad (\text{S20})$$

Then, the perfect shuffling can be decomposed as $f^{(2N)} = f_{m,m-1}^{(2N)} \dots f_{2,1}^{(2N)} \cdot f_{1,0}^{(2N)}$ because

$$\begin{aligned} f_{m,m-1}^{(2N)} \dots f_{2,1}^{(2N)} \cdot f_{1,0}^{(2N)}([b_m b_{m-1} \dots b_2 b_1 b_0]_2) &= f_{m,m-1}^{(2N)} \dots f_{2,1}^{(2N)}([b_m b_{m-1} \dots b_2 \mathbf{b}_0 b_1]_2) \\ &= f_{m,m-1}^{(2N)} \dots f_{3,2}^{(2N)}([b_m b_{m-1} \dots \mathbf{b}_0 b_2 b_1]_2) \\ &\vdots \\ &= [\mathbf{b}_0 b_m b_{m-1} \dots b_2 b_1]_2 \\ &= f^{(2N)}([b_m b_{m-1} \dots b_2 b_1 b_0]_2) \end{aligned} \quad (\text{S21})$$

(Note that \mathbf{b}_0 is displaced to the left by one site in each application of $f_{i+1,i}^{(2N)}$.) Observe that the function $f_{i,j}^{(2N)}$ maps an input integer $\dots b_i \dots b_j \dots$ to itself if $b_i = b_j$ and to some other integer if $b_i \neq b_j$. Also, two sequential applications of $f_{i,j}^{(2N)}$ yield an

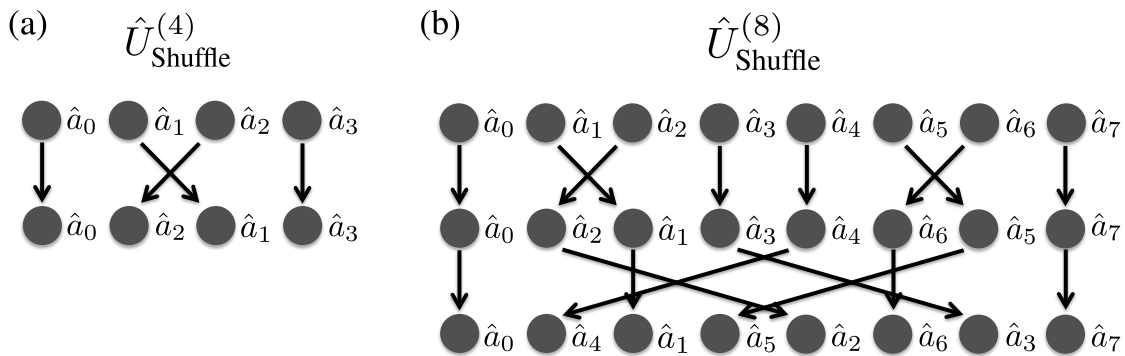


FIG. S2: Examples of the $2N$ -mode perfect shuffling circuits in circuit depth $\log_2 N$ with $\frac{N}{2} \log_2 N$ two-mode SWAP operations.

identity operation. Thus, there are N input integers that are invariant under the action of $f_{i,j}^{(2N)}$ and $N/2$ pairs of N input integers that are exchanged with their paired partner under $f_{i,j}^{(2N)}$. In other words, $f_{i,j}^{(2N)}$ corresponds to a simultaneous application of $N/2$ non-overlapping two-mode SWAP operations. The decomposition in Eq. (S21) then implies that the $2N$ -mode perfect shuffling can be implemented by $\frac{N}{2} \log_2 N$ two-mode SWAP operations in depth $m = \log_2 N$ where each layer contains $\frac{N}{2}$ simultaneous separate two-mode SWAP operations (see Fig. S2 for examples with $N = 2, 4$).

Thus, denoting by $D(N)$ the minimum circuit depth to implement the N -mode Gaussian transformation, we have

$$D(2N) \leq D(N) + c \log_2 N, \quad (\text{S22})$$

for some constant $c > 0$ (which can be chosen to be 4) and $N \geq 2$. Using $D(2) = 2$ and mathematical induction, one can show

$$D(N) \leq c((\log_2 N)^2) = \mathcal{O}((\log N)^2). \quad (\text{S23})$$

In this case, however, one needs to perform $\frac{N}{2} \log_2 N$ two-mode SWAP operations to implement the $2N$ -mode perfect shuffling, as opposed to the $2N$ two-mode SWAP operations in the unparallelized case. Thus, the required total number of single- and two-mode operations scales as $\mathcal{O}(N(\log N)^2)$, as can be shown by replacing cN by $cN \log_2 N$ in Eq. (S17).
